Structure and visible photoluminescence of porous $Si_{1-x}Ge_x$

M. Schoisswohl, J. L. Cantin, M. Chamarro, and H. J. von Bardeleben
Groupe de Physique des Solides, Universités Paris 6&7, URA 17 au CNRS, 2 place Jussieu, 75005 Paris, France

T. Morgenstern, E. Bugiel, and W. Kissinger
Institute of Semiconductor Physics, P.O. Box 409, D-15204 Frankfurt (Oder), Germany

R. C. Andreu
Fisica de la Materia Condensada, Facultad de Ciencias, Universidad-Zaragossa, Plaza San Francisco s/n, 50009 Zaragoza, Spain
(Received 10 April 1995)

Porous $Si_{1-x}Ge_x$ layers with efficient room-temperature visible photoluminescence (PL) were elaborated by anodical etching from p- and p^+-type doped epitaxial layers with Ge contents of 5% and 20%. The luminescence is characterized by a broad PL band centered at 650 nm, similar to the case of porous Si; its width and spectral dependence vary only slightly with the Ge composition. Time-resolved PL spectra reveal lifetimes in the 10^2-ns range decreasing with increasing Ge concentration. The pore structure of the p^+-type layers has typical dimensions in the 50–100 Å range and is [100] oriented. Electron paramagnetic resonance results show the presence of Si- and Ge-P_b centers as well as Si and Ge dangling-bond centers, the relative concentrations of which depend on the porosity and the surface passivation state. The angular variation of the Si- and Ge-P_b center electron paramagnetic resonance spectra demonstrate the crystallinity of the porous SiGe layers.

I. INTRODUCTION

Porous Si (PS) has been shown to be a complex semiconductor material with optical and electrical properties distinct from bulk Si. In particular, high-porosity (>70%) PS shows efficient room-temperature visible photoluminescence (PL). The origin of the visible photoluminescence has been the object of numerous studies.[1–4] It is generally attributed to the presence of nanocrystals with nm dimensions giving rise to quantum confinement effects and/or the presence of surface states. The wide interest in the visible PL of porous silicon is motivated by both the fundamental interest in the electronic structure of a system of interconnected nanocrystals as well as by potential technological applications. Indeed, PS might lead to the fabrication of all-silicon-based optoelectronic devices, functioning in the visible spectral range. One major drawback for optoelectronic applications is the long radiative lifetime, which is in the μs range at room temperature, in agreement with theoretical predictions for excitonic recombination in Si nanocrystals.[4]

Porous semiconductors based on alloy systems might be alternative and as concerns PL efficiency and lifetime potentially more interesting materials for optoelectronic applications, but have not been studied widely up to now. In particular the SiGe alloy system seems to be promising: the incorporation of Ge atoms in Si nanocrystals is expected to reduce the lifetime for exciton recombination and to increase the radiative recombination efficiency.[5] However, only very few experimental studies of porous SiGe have been reported up to now.[6–8] Most of them were performed on porous SiGe prepared by a stain etching, which had given rise to the formation of highly disordered or amorphous material,[7] the properties of which cannot be directly compared to those of monocrystalline porous SiGe.

In this study we have prepared porous SiGe by anodic dissolution of SiGe/Si epitaxial layers. The layers have been characterized by electron microscopy and electron paramagnetic resonance spectroscopy. Both continuous and time-resolved PL of the observed visible emission have been studied as a function of Ge content, doping, and surface passivation. Our results confirm the high potential as visible light-emitting material of porous SiGe, which is obtained by anodic dissolution in the form of monocrystalline porous layers with efficient orange room-temperature photoluminescence.

II. EXPERIMENT

Boron-doped SiGe layers of thicknesses between 500 and 2000 nm and Ge contents of 5% and 20% were grown by low-pressure chemical vapor deposition on (100)Si substrates using a standard Si-epitaxy horizontal tube reactor. The layers had a typical oxygen content of 10^{19} cm^{-3}. Two different doping concentrations, p ($[B]\approx 10^{17}$ cm^{-3}) and p^+ ($[B]>10^{19}$ cm^{-3}), expected to give rise to different pore structures, were chosen. Porous layers were prepared by anodical etching in a $HF/C_2H_5OH/H_2O$ electrolyte with HF concentrations between 12.5 and 24 vol. %. The currents used were between 10 and 40 mA/cm^2, adapted to obtain porosities in the 70% range. The actual porosity of the layers has been estimated from gravimetric measurements. Fresh, as-prepared samples, as well as room-temperature aged ($\approx$6 months) samples and low-temperature (300 °C) thermally oxidized samples have been studied.

The morphology of the layers was investigated by electron microscopy [scanning (SEM) and transmission (TEM)] and by electron paramagnetic resonance (EPR)

0163-1829/95/52(16)/11898(6)/$06.00

measurements. The EPR measurements have been performed with an X-band spectrometer. Typical sample dimensions are 3×6 mm^2. Most of the EPR measurements have been done on single samples at room temperature.

The continuous and time-resolved PL measurements were carried out at room temperature using Ar and N_2 laser pumped dye lasers, respectively. The laser power was limited to less than 600 mW cm^{-2} to eliminate PL fatigue phenomena during the PL measurements. The excitation spectrum of the visible PL was measured with a halogen lamp.

III. THE MORPHOLOGY OF THE p^+- AND p-TYPE LAYERS

Figure 1 shows a typical SEM photography of an anodically etched p^+-type $Si_{0.8}Ge_{0.2}$ layer. The sample contains three different regions: $a\approx1$-μm-thick top layer of porous SiGe formed by the anodical etching process, an underlying bulk SiGe epitaxial layer, and beneath the Si substrate. The TEM images reveal clearly the formation of a columnlike pore structure of the porous SiGe layer with a structure closely analogous to that observed in p^+-type porous Si of comparable porosity.[9,10] The columns are [001] oriented and the etching front is parallel to the surface of the remaining SiGe layer. Typical pore dimensions, observable at higher resolution (Fig. 2), are 10 nm and the remaining SiGe skeleton has a diameter of typically 5 nm. The existence of a local substructure with lower dimensions must be evoked to explain the visible PL within the quantum confinement model in these layers. The porosity determined from the gravimetric method is estimated to 50%. The electron microscopy results show the influence of dislocations on the porous/bulk interface structure: the etching, which leads to a flat interface in the case of Si, is increased at dislocations extending some 10 nm deeper into the epitaxial layer. A top view of the pore structure of a p-type doped SiGe layer is given in Fig. 3. The pore dimensions are similar to those observed in the p^+type doped layers. In contrast to the p^+ material we find here a spongelike structure of the porous SiGe layers similar to the case of p-type porous Si.[11]

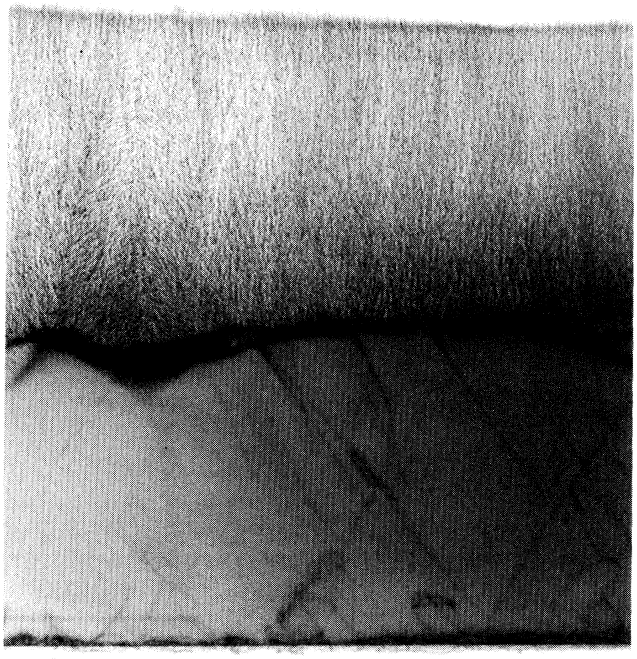

FIG. 1. TEM image of a porous p^+-type SiGe sample. The photo shows the Si substrate below, the nonattacked $Si_{0.8}Ge_{0.2}$ and the porous $Si_{0.8}Ge_{0.2}$ layer. The porosity was estimated to 50%. The lateral dimensions of the image correspond to 1.9×2.3 μm.

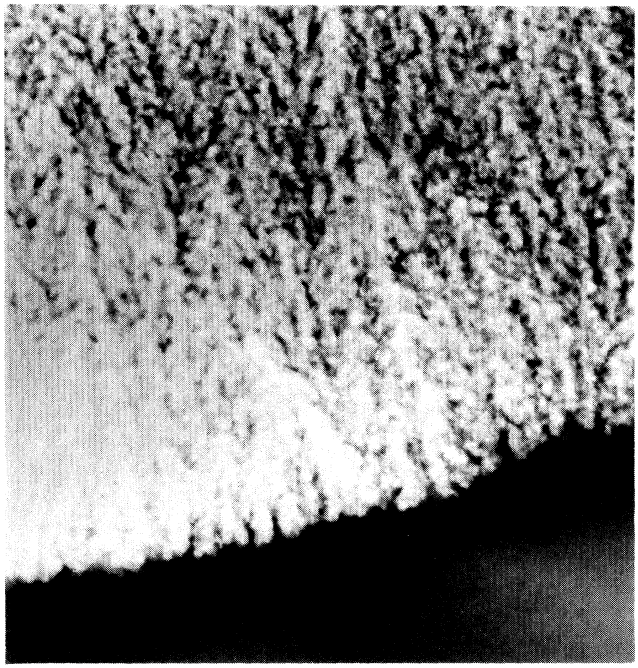

FIG. 2. High-resolution TEM image of the interface p^+ $Si_{0.8}Ge_{0.2}$, porous $Si_{0.8}Ge_{0.2}$ showing the skeleton structure of the porous layer. The sample section shown corresponds to 450×500 nm.

FIG. 3. SEM image of the top view of a p-type $Si_{0.95}Ge_{0.05}$ layer. The width of the shown sample area corresponds to 2 μm.

Previous EPR studied on porous Si layers have shown the interest of such studies for a global defect and structure analysis.[12,13] The dominant paramagnetic defect detected in PS has been the P_b center, which is generally attributed to the neutral Si dangling-bond defect at the Si/SiO_2 interface. The angular variation of the P_b center EPR spectrum is a sensitive probe for the monocrystalline, strained, and disordered character of the porous layers.[14] Defects have equally been detected in the oxide layer (E').[15] The P_b and E' centers are electrically active and thus can trap carriers and modify the recombination processes of photocarriers. The concentration of the P_b centers is strongly dependent on the oxidation state of the internal surfaces. Perfect hydrogen-passivated surfaces will not contain P_b centers. To our knowledge, no previous EPR results on interface or volume defects in SiGe layers have been reported with the exception of SIMOX (silicon implanted with oxygen) material. For SIMOX SiGe layers of 10% and 40% Ge two spectra (SG1) with slightly different g values had been observed, which were both tentatively attributed to the Ge P_b center at the oxide interface. The g factors of the SG1 defect are Ge composition dependent.[16,17]

Room-temperature EPR studies on as-prepared porous SiGe samples show as in the case of porous Si layers the presence of an anisotropic spectrum, the properties of which are compatible with the Si P_b and P_{b0} dangling-bond interface defects. However, the signal-to-noise ratio is too low due to the small fraction of the oxidized surface in the as-prepared state and the small layer thickness (0.5–1 μm) to allow a quantitative analysis. To increase the spin concentration we have submitted the samples to low-temperature (300 °C) oxidation. Previous Rutherford backscattering studies on porous Si had shown that the oxidation step at 300 °C leads to the formation of very thin oxide layers of about 2 ML.[18] After the 300 °C oxidation various EPR spectra were observed. The occurrence of the spectra depends on the porosity of the samples:

The high-porosity samples are characterized by the dominant presence of the trigonal Si P_b center, which is characterized by the Landé g factors $g_{\parallel}=2.0022\pm0.0002$ and $g_{\perp}=2.0084\pm0.0002$ (see Figs. 4 and 5). The linewidth of the EPR spectrum shows an angular dependence with a lowest value of 1.8 G for $B\|[111]$ and a maximum value of 2.8 G for $B\|[110]$. The angular dependence of the Si P_b center spectrum gives no evidence for disordering of the porous SiGe layer. If amorphous or strongly disordered inclusions were present in these layers we would expect the observation of the averaged P_b center spectrum giving rise to an isotropic line at $g=2.006$. Such a spectrum is not observed. We do, however, observe an isotropic line at $g=2.019\pm0.0005$ with a linewidth of more than 30 G [Fig. 4(a)]. The g factor and linewidth are characteristic for a Ge dangling-bond defect, a defect previously studied in amorphous Ge.[16] The simultaneous presence of an unperturbed Si P_b center spectrum and the Ge dangling-bond spectrum is ascribed to the formation of Ge precipitates at the $SiGe/SiO_2$ interface or in the SiO_2 layer.

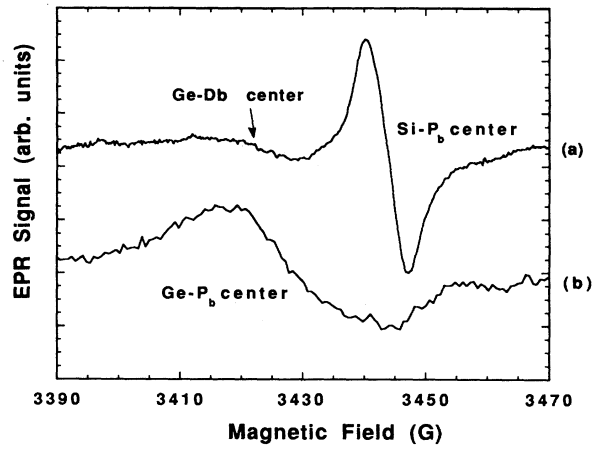

FIG. 4. Room-temperature EPR spectra of a high- (a) and a low- (b) porosity p^+-type $Si_{0.8}Ge_{0.2}$ layer.

The second type of porous $Si_{0.80}Ge_{0.20}$ layer, of medium porosity, shows after the same 300 °C oxidation treatment the Si P_b center EPR spectrum and in addition a second anisotropic spectrum, the angular variation of which is given in Fig. 6. The EPR spectrum is characteristic of a defect with trigonal point symmetry, electron spin $S=\frac{1}{2}$ and an axially symmetric g tensor with principal values $g_{\parallel}=2.0008\pm0.0005$ and $g_{\perp}=2.0210\pm0.0005$. The linewidth of the EPR spectra is orientation dependent and varies from 20 G for $B\|[111]$ to 32 G for $B\perp[111]$. This EPR spectrum is attributed to the Ge P_b center in porous $Si_{0.80}Ge_{0.20}$. More details of this spectrum will be given in another paper. The isotropic Ge dangling-bond spectrum is not observed in these samples.

It is further instructive to compare the neutral Si and Ge P_b center concentrations. If the concentrations of the interface defect were independent of the chemical nature of the interface atoms we would expect defect ratios of $[Pb_{Ge}]/[Pb_{Si}]=0.2/0.8=1/4$. The experimentally found concentration ratios do not correspond to the value of $\frac{1}{4}$ and are >10. A simple model explaining this result is

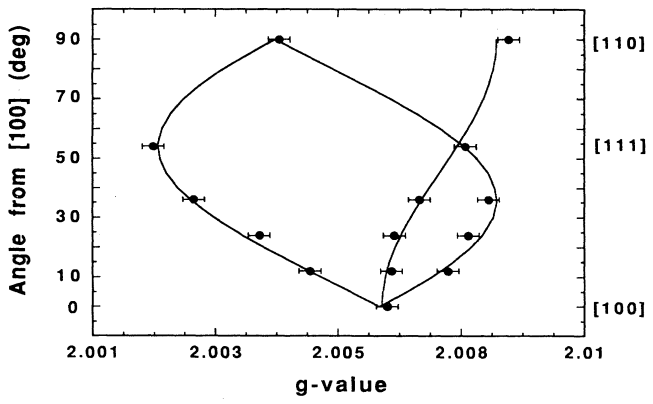

FIG. 5. Angular variation of the Si P_b center EPR spectrum in 300 °C oxidized highly porous p^+-type $Si_{0.8}Ge_{0.2}$ with g values of $g_{\parallel}=2.0022\pm0.0002$ and $g_{\perp}=2.0084\pm0.0002$.

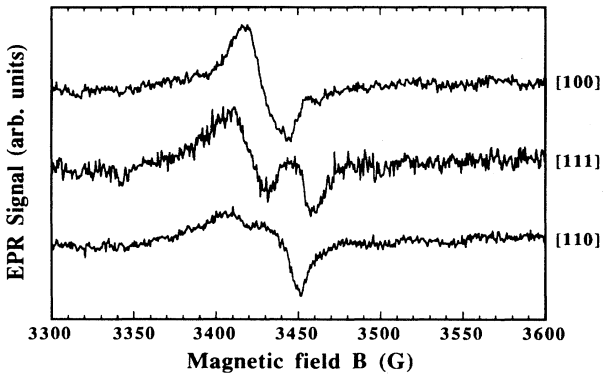

FIG. 6. Angular variation of EPR spectra of the Ge P_b center in a low-porosity p^+-type $Si_{0.8}Ge_{0.2}$ layer; the spectra of the Si P_b center are subtracted.

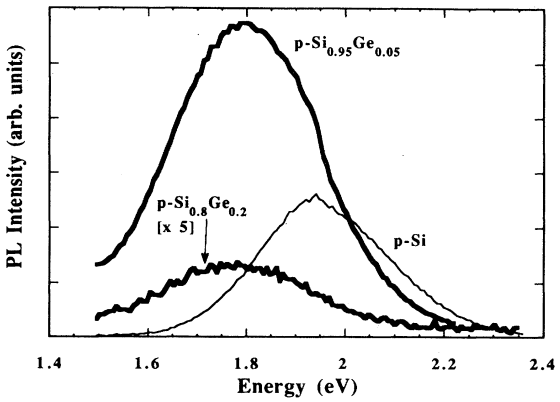

FIG. 7. Comparison of the PL between porous Si and SiGe with 5% and 20% Ge content obtained by excitation with 488 nm and a power density of less than 300 mW cm^{-2}. All samples were prepared with the same conditions.

the following: in low-porosity SiGe thermal oxidation proceeds without perturbation of the interface stoichiometry, but only Si surface atoms are able to form oxygen bonds. In such a configuration for (111) interfaces a "normal" Si P_b center concentration is about 10^{13} cm^{-2}, corresponding to 1% of the interface sites, but a Ge P_b center concentration of 0.2×10^{15} cm^{-2} would be expected. This model is in agreement with previous oxidation results of nonporous SiGe.[19] In the case of high-porosity oxidized SiGe layers however, the Ge atom at the interface precipitate and give rise to a local $Si/Ge/SiO_2$ structure.

IV. PL MEASUREMENTS

A. cw PL measurements

All high-porosity SiGe samples, irrespective of the 5% or 20% Ge content and doping concentrations, show a broad visible PL band centered at ≈ 1.8 eV at room temperature. Figure 7 shows the PL spectra obtained from the porous SiGe layers excited with the 488-nm line of an Ar laser. This figure contains also the PL spectrum of a porous p-type Si layer prepared with the same etching conditions. The maximum of the PL band is shifted by ≈ 0.2 eV to lower energies as compared to PS; this shift depends on the porosity and the age/oxidation state of the samples. No simple correlation with the alloy composition and band structure seems to be possible at this stage. Our results do not confirm the measurements of Gardelis *et al.*, who had observed a strong blueshift of about 0.3 eV for porous SiGe as compared to porous Si.[6] The PL intensity of the 5% Ge content samples has been observed to be higher than that for porous Si by a factor of 3 and for the 20% Ge layer the PL intensity is reduced by an order of magnitude, as can be seen also in Fig. 7. It has to be mentioned that depending on the etching condition and the aging stage of the samples we observed in the 20% Ge samples PL intensities comparable to those of the 5% Ge layers.

We have further investigated the qualitative influence of the doping concentration and the etching parameters on the visible PL spectrum of as-prepared layers. The following main features have been observed. First, we found PL intensities of the same order of magnitude for p- and p^+-type porous $Si_{0.8}Ge_{0.2}$ layers whereas the variations observed in porous Si (Refs. 3 and 21) are much more important. A comparison of samples prepared with different current densities between 20 and 40 mA/cm^2, using the same etching solutions and times and having exactly the same age (2 months) reveal that the PL intensity of the porous SiGe increases with increasing current density and saturates at high current density. The line shape and position of the PL spectrum were not influenced by the change in the current density.

In order to obtain further insight on the luminescence, the excitation spectrum of the visible PL at 630 nm has been measured (Fig. 8). Within the spectral range of 2.1 to 4 eV we find an exponential tail region, followed by a plateau between 3 and 4 eV. The spectrum is similar to that obtained on p-type porous Si.[20]

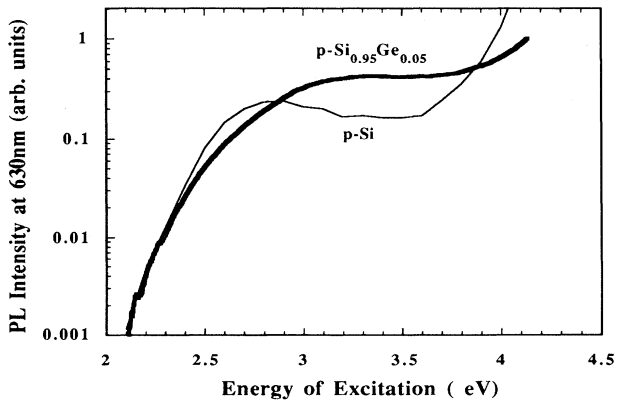

FIG. 8. Excitation spectra of a p-type $Si_{0.95}Ge_{0.05}$ layer. The spectra are corrected for the instrumental response and compared to p-Si after Ref. 20.

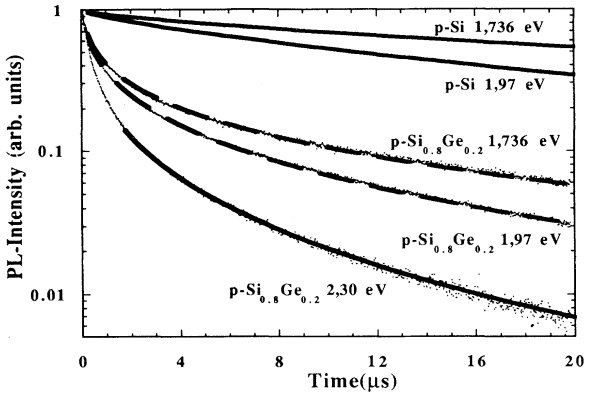

FIG. 9. Time decay for different wavelengths of porous *p*-type $Si_{0.8}Ge_{0.2}$ in comparison with the values found for porous *p*-type Si in the literature (Ref. 23).

B. Time-resolved PL measurements

In porous Si the lifetime of the dominant red PL, at room temperature, is slow in the region of 100 μs to some 10 μs.[22–24] We have investigated the room-temperature decays of the red PL in porous SiGe. The results are shown in Fig. 9 for several detection energies and compared to the decays of porous Si, found in the literature. The decay of the PL depends on the detection energy showing a shortening of the decays with increasing detection energies. In any case the decay of the SiGe is faster than that previously observed on porous Si. The time dependence of the PL decay in porous SiGe is nonexponential and can be very well fitted by a stretched exponential decay function of the form

$$I(t)=I(0)\exp(-t/\tau)^{\beta},$$

where τ is a mean lifetime and β a nonexponential factor taking into account a broad lifetime distribution. Figure 10 gives the values for τ and β as a function of the Ge content. For the 1.73- and 1.97-eV lines we obtained in our porous $Si_{0.8}Ge_{0.2}$ lifetimes of some 100 ns, which is at least a factor of ≈ 50 lower than that of porous Si; at an energy of 2.3 eV, which is still part of the broad red emission band the deduced lifetime is 95 ns. Also the values for the stretching exponent β, obtained from the fit, showed a decrease from about 0.74 (Ref. 22) for porous Si to values between 0.263 and 0.371 for porous $Si_{0.8}Ge_{0.2}$.

In summary, our PL results on SiGe samples show that the effect of alloying for small alloy concentrations ($<20\%$) has only negligible influence on the spectral dependence of the visible PL spectrum. This can be easily understood by the small effect on the change in band structure as compared to the change induced by quantum confinement effects as well as by the fact that the passivating oxide layer is in both cases of porous Si and porous SiGe only composed of SiO_2. The lifetime and radiative efficiency are, however, strongly influenced by the alloying effect.

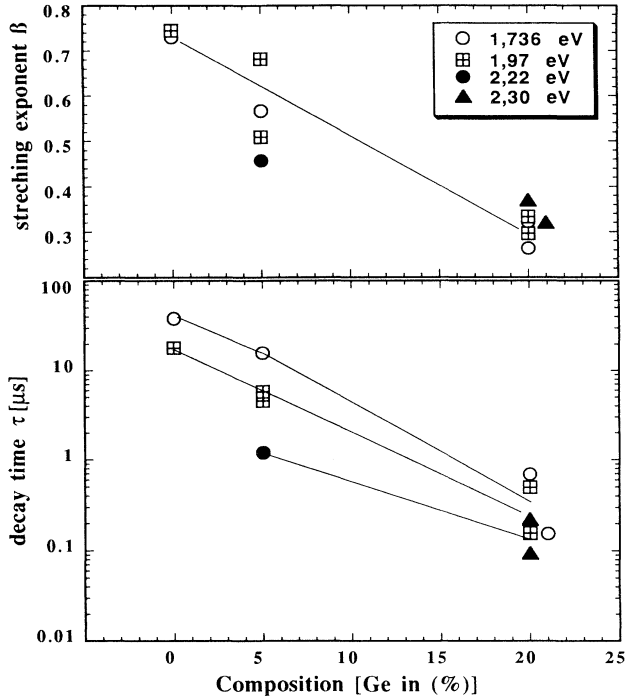

FIG. 10. PL decay time τ and stretching exponent β for *p*-type porous SiGe layers in comparison with porous *p*-type Si from the literature (Ref. 23). The indicated lines are guides to the eye. The legend is valid for both graphs.

V. CONCLUSION

Porous semiconductors based on the SiGe alloy system have been shown to be promising extensions of the porous Si system, which has been mainly studied up to now; improved optical PL properties, concerning PL efficiency and PL lifetime of the main red emission band, can be achieved without loss of the monocrystalline character of the porous layers. Porous SiGe is equally another material support for $SiGe/SiO_2$ interface defect studies, which have only been marginally studied up to now by the electron paramagnetic resonance technique due to insufficient spin concentrations in bulk samples.

[1]J. C. Vial, A. Bsiesy, F. Gaspard, R. Hérino, M. Ligeon, F. Muller, and R. Romestain, Phys. Rev. B **45**, 14 171 (1992).

[2]A. G. Cullis, L. T. Canham, G. M. Williams, P. W. Smith, and O. D. Dosser, J. Appl. Phys. **75**, 493 (1994).

[3]G. Bomchil, A. Halimaoui, I. Sagnes, P. A. Dadoz, I. Berbezier, P. Perret, B. Lambert, G. Vincent, L. Garchery, and J. L. Regolini, Appl. Surf. Sci. **65/66**, 394 (1993).

[4]C. Delerue, G. Allan, and M. Lannoo, Phys. Rev. B **48**, 11 024 (1993).

[5]M. Lannoo (private communication).

[6]S. Gardelis, J. S. Rimmer, P. Dawson, B. Hamilton, R. A. Kubiak, T. E. Whall, and E. H. C. Parker, Appl. Phys. Lett. **59**,

2118 (1991).
[7]W. T. Pike, A. Ksendzov, R. W. Fathauer, and T. George, J. Vac. Sci. Technol. B **11**, 1401 (1993).
[8]Y. Kolic, E. Borne, M. A. Garcia Perez, A. Sibai, R. Gauthier, and A. Laugier, Thin Solid Films **255**, 279 (1995).
[9]S. F. Chuang, S. D. Collins, and R. L. Smith, Appl. Phys. Lett. **55**, 675 (1989).
[10]H. Sugiyama and O. Nittono, Jpn. J. Appl. Phys. **28**, L2013 (1989).
[11]P. C. Searson, J. M. Macaulay, and S. M. Prokes, J. Electrochem. Soc. **139**, 3373 (1992).
[12]H. J. von Bardeleben, D. Stievenard, A. Grosman, C. Ortega, and J. Siejka, Phys. Rev. B **47**, 10 899 (1993).
[13]M. Schoisswohl, H. J. von Bardeleben, V. Morazzani, A. Grosman, C. Ortega, St. Fronhoff, M. G. Berger, and H. Münder, Thin Solid Films **225**, 123 (1995).
[14]A. Stesmans, Phys. Rev. B **48**, 2418 (1993).
[15]H. J. von Bardeleben, C. Ortega, A. Grosman, V. Morazzani, J. Siejka, and D. Stievenard, J. Lumin. **57**, 301 (1993).
[16]M. E. Zvanut, W. E. Carlos, M. E. Twigg, R. E. Stahlbush, and D. J. Godbey, Mater. Sci. Forum **83-87**, 1493 (1992).
[17]M. E. Zvanut, W. E. Carlos, M. E. Twigg, R. E. Stahlbuch, and D. J. Godbey, J. Vac. Sci. Technol. B **10**, 2026 (1992).
[18]V. Morazzani, M. Chamarro, A. Grosman, C. Ortega, S. Rigo, J. Siejka, and H. J. von Bardeleben, J. Lumin. **57**, 45 (1993).
[19]C. Caragianis, Y. Shigesato, and D. C. Paine, J. Electron. Mater. **23**, 883 (1994).
[20]L. Wang, M. T. Wilson, and N. M. Haegel, Appl. Phys. Lett. **62**, 1113 (1993).
[21]M. Schoisswohl, H. J. von Bardeleben, V. Bratus, and H. Münder, Thin Solid Films **255**, 163 (1995).
[22]N. Y. Kanemitsu, Phys. Rev. B **48**, 12 357 (1993).
[23]I. Pavesi and M. Ceschini, Phys. Rev. B **48**, 17 625 (1993).
[24]Y. H. Xie, M. S. Hybertsen, W. L. Wilson, S. A. Ipri, G. E. Carver, W. L. Brown, E. Dons, E. E. Weir, A. R. Kortan, G. P. Watson, and A. J. Liddle, Phys. Rev. B **49**, 5386 (1994).

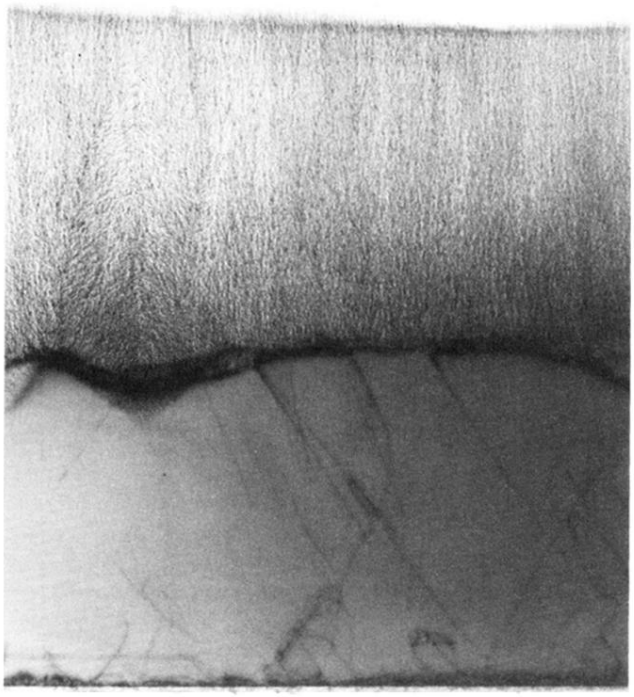

FIG. 1. TEM image of a porous p^+-type SiGe sample. The photo shows the Si substrate below, the nonattacked $Si_{0.8}Ge_{0.2}$ and the porous $Si_{0.8}Ge_{0.2}$ layer. The porosity was estimated to 50%. The lateral dimensions of the image correspond to $1.9 \times 2.3\ \mu m$.

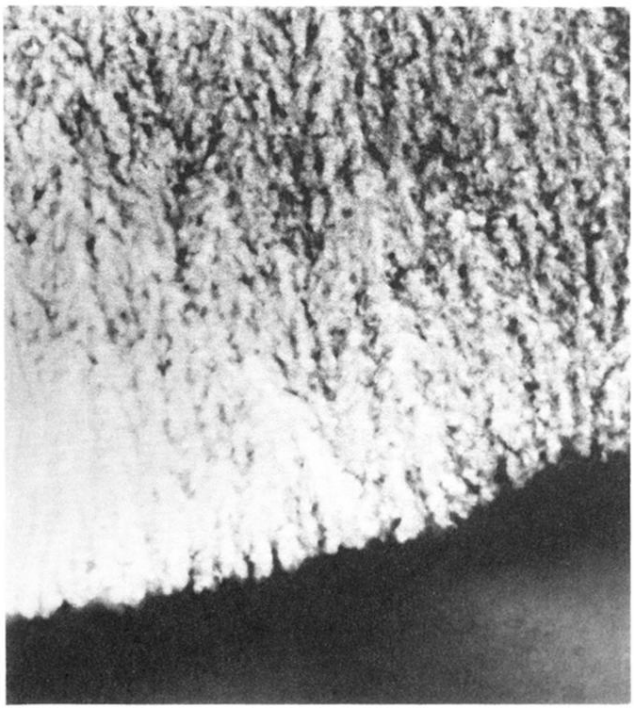

FIG. 2. High-resolution TEM image of the interface p^+ $Si_{0.8}Ge_{0.2}$, porous $Si_{0.8}Ge_{0.2}$ showing the skeleton structure of the porous layer. The sample section shown corresponds to 450×500 nm.

FIG. 3. SEM image of the top view of a p-type $Si_{0.95}Ge_{0.05}$ layer. The width of the shown sample area corresponds to 2 μm.